Chemical Interactions in the Surface-Enhanced Resonance Raman Scattering of Ruthenium Polypyridyl Complexes

Bruce D. Alexander[†] and Trevor J. Dines*

Division of Physical and Inorganic Chemistry, Carnelley Building, University of Dundee, Dundee, DD1 4HN, U.K.

Received: April 1, 2004; In Final Form: August 31, 2004

Surface-enhanced resonance Raman scattering (SERRS) from the α-diimine complexes $[Ru(bpm)_3]^{2+}$ and $[Ru(bpz)_3]^{2+}$ is reported for the first time at a roughened silver electrode. In both cases, a possible adsorbate orientation has been proposed involving binding through nitrogen lone pair electrons to the silver surface, based on changes in band positions upon adsorption. The SERRS spectra of $[Ru(bpm)_3]^{2+}$ were found to change slightly with a change in applied potential. The relative intensity of the ν(C6C6′) band was found to be dependent on both excitation wavelength and applied potential. This was ascribed to an active charge transfer (CT) mechanism operating synergistically with the electromagnetic mechanism. No such CT activity was observed in $[Ru(bpz)_3]^{2+}$. It is tentatively suggested that this behavior may arise from the different modes of adsorption of the two complexes.

Introduction

The ubiquity of transition-metal complexes with α-diimine ligands, such as 2,2′-bipyridine (bpy), 2,2′-bipyrimidine (bpm), or 2,2′-bipyrazine (bpz), owes largely to the versatility of both the ligands and their resulting complexes. Aside from their continuing importance in dye-sensitized solar cells,[1,2] such complexes are increasingly important to the applications of thin-film organic light-emitting diodes (OLEDs),[3] biosensors,[4,5] and as mediators in studies of electron transfer in DNA.[6] While such synthetic flexibility is undoubtedly valuable when tailoring the photophysical and photochemical properties of the system of interest, it also provides a means to study adsorption processes and interactions between complexes and electrode surfaces, not only crucial for OLEDs and dye-sensitized solar cells but also for a more fundamental understanding of the mechanisms involved in the surface-enhanced Raman spectroscopy (SERS) process.

Discovered some 30 years ago,[7,8] SERS is not a new technique. The power of the technique has already been proven in a number of analytical fields, most notably in those of genetic analysis,[9−11] detection of illicit drugs,[12] detection of explosives,[13,14] and forensic science.[15,16] The age and apparent popularity of the technique may lead one to believe that the mechanisms responsible for the SERS effect were fully resolved and understood. In fact, this is not strictly the case. It seemed likely that the SERS effect arose from two different, multiplicative mechanisms, commonly termed the electromagnetic (EM) mechanism and the chemical mechanism. The EM mechanism was found to be dominant and is generally regarded as arising from an enhancement of both the excitation and scattered radiation due to electromagnetic resonance between the excitation/scattered light and the free electrons residing in localized surface features.[17] The weaker chemical mechanism remains much more enigmatic and difficult to ascertain. It has already been pointed out that the term "chemical mechanism" is rather a broad church designed to house all of the mechanisms proposed to exist in order to explain anomalies between experimental data and the EM mechanism such as changes in relative intensities at different applied potentials and the fact that enormous enhancement factors are observed for some molecules but others show only small enhancement, if any at all.[18,19] Of these mechanisms, it is the charge-transfer (CT) mechanism that seems most able to describe the dependence of the relative intensities with the applied potential of certain bands in the SERS spectra of species adsorbed on electrode surfaces in absence of molecular reorientation.[20,21] Indeed, a large base of modeling work designed to verify the existence of the CT mechanism has been reported albeit on a rather narrow range of molecules.[22−24]

The CT mechanism proposed by Lombardi et al.[20] suggests that a surface complex is formed between the electrode surface and the adsorbate. Upon formation, it is possible to excite a resonance Raman-like process involving the electronic orbitals of the adsorbate and the conduction band of the metal. Variation of applied potential would then change the position of the conduction band, and so the surface-based resonance Raman-like process could be tuned into and out of resonance with the incident irradiation, thus giving a potential at which certain bands involved in this process attain maximum relative intensity, V_{max}. How this potential of maximum relative intensity behaves with respect to the excitation energy would then indicate the nature of the resonance Raman-like process, i.e., whether there is a charge transfer from adsorbate to metal or vice versa. Yet despite this model offering a way of explaining the phenomenon present at an electrode surface, it remains controversial. Its existence has rarely been directly detected, notably by Campion and co-workers,[19,25−28] but seldom unequivocally.[29] There still remains a strong need to explain the dependence of certain SERS spectra on applied potentials.

Despite this, SERS has received yet another new lease of life with the discovery of single-molecule SERS facilitating

* To whom correspondence should be addressed. E-mail: t.j.dines@dundee.ac.uk. Fax: 44-1382-345517.

[†] Present address: Département de Chimie Minérale, Analytique et Appliquée, University of Geneva, Sciences II, 30 quai E.-Ansermet, 1211 Geneva, CH. E-mail: bruce.alexander@chiam.unige.ch.

10.1021/jp0485690 CCC: $30.25
Published on Web 02/05/2005

ultralow detection levels, which clearly fit perfectly the demands of biochemical analysis.[30−33] However, with this advance has come yet more controversy regarding the mechanisms responsible for the phenomenon. It should be clarified that the current paper concerns itself not with the recent fashion for "hot spots" or "blinking" spectra, such problems relating specifically to single-molecule detection; rather, it is aimed at evaluating the validity of the chemical mechanism in the traditional ensemble-averaged regime: such mechanisms are currently more relevant to the spectroelectrochemist. It is proposed that a change in the position of aromatic nitrogen atoms may be sufficient to induce a quantifiable difference in the behavior of the SERS spectra with respect to applied potential of two isomers. The authors report for the first time the SERS spectra of $[Ru(bpm)_3]^{2+}$ and $[Ru(bpz)_3]^{2+}$, and their differences are discussed within traditional ensemble-average surface enhancement models, the validity of which is also discussed.

Experimental Section

Both $Ru(bpm)_3Cl_2$ and $Ru(bpz)_3Cl_2$ were prepared following a reflux of the appropriate ligand with $Ru(DMSO)_4Cl_2$ in water according to literature methods.[34,35] 2,2′-Bipyrimidine was commercially available (Aldrich). 2,2′-Bipyrazine was prepared by the pyrolysis of bis(2-pyrazinecarboxylato)copper(II) under a nitrogen atmosphere;[35] $Ru(DMSO)_4Cl_2$ was obtained after reflux of $RuCl_3$ in DMSO.[36] All products were characterized by ^1H NMR and electronic absorption spectroscopies.

IR spectra were recorded using 1% (w/w) pressed KBr disks in a Perkin-Elmer Spectrum One Fourier Transform (FT) spectrometer with a resolution of 4 cm^{-1}. The FT IR spectrometer was fitted with a deuterated triglycerine sulfate detector and KBr beam splitter. Resonance Raman (RR) and surface enhanced resonance Raman (SERRS) spectra were obtained using excitation in the 457.9−514.5 nm range using a Spectra-Physics Series 2000 argon ion laser. Power at the laser head did not exceed 100 mW. Scattered radiation was dispersed using a Spex 1403 spectrometer equipped with a Hamamatsu R928 photomultiplier detector. Spectral resolution was typically of the order of 4 cm^{-1}.

SERRS spectra were recorded from the surface of a polycrystalline silver electrode housed in a Teflon cell fitted with quartz windows. Platinum wire was used as a counterelectrode along with a Ag/AgCl reference electrode. All potentials are reported vs Ag/AgCl. Potentiostatic control was provided by an EcoChimie μAutolab potentiostat. The silver electrode was first polished mechanically with a Al_2O_3 slurry to a mirrorlike finish before being rinsed thoroughly with deionized water. Activation of the electrode was then performed by electrochemically roughening with 10 oxidation−reduction cycles between the potentials of 400 and −600 mV at a scan rate of 0.1 V s^{-1} in a 0.1 mol dm^{-3} KCl solution that had been thoroughly degassed.

Results and Discussion

The ab initio molecular modeling of the vibrational spectra and scaled quantum mechanical normal coordinate analysis (SQM-NCA) of $[Ru(bpm)_3]^{2+}$ and $[Ru(bpz)_3]^{2+}$ have been recently reported by Alexander and Dines.[37] Atom numbering, assignments, and descriptions of the normal modes reported herein follow those of this previous report. Both $Ru(bpm)_3Cl_2$ and $Ru(bpz)_3Cl_2$ were optimized assuming D_3 symmetry and treated as $[Ru(bpm)_3]^{2+}$ and $[Ru(bpm)_3]^{2+}$ dications by ignoring the Cl^- counterions. Calculations of vibrational band positions and IR intensities were performed using the Gaussian 98 program[38] at the B3-LYP/LanL2DZ level, whereas Raman activities were calculated at the HF-SCF/LanL2DZ level. The LanL2DZ basis set is an effective core potential basis set and was shown to be highly efficient for the calculation of vibrational spectra of systems with a large number of electrons such as those of the present report. Scaled normal coordinate analysis performed followed the scaling method of Pulay.[39] A scale factor of 0.90 was applied to all force constants concerning motion of the hydrogen atoms, and a scale factor of 1.025 was applied to all other force constants. Both $[Ru(bpm)_3]^{2+}$ and $[Ru(bpz)_3]^{2+}$ contain 55 atoms, thus there are 159 normal modes, which transform under D_3 symmetry as $\Gamma_{3N-6} = 27a_1 + 26a_2 + 53e$. Modes transforming as a_1 or e are Raman active, whereas those transforming as a_2 or e are IR active.

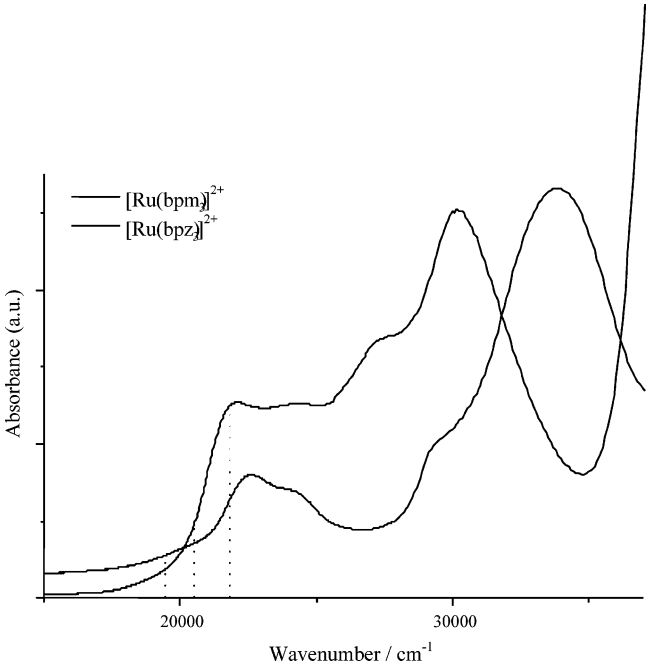

Figure 1. Electronic absorption spectra of $[Ru(bpm)_3]^{2+}$ and $[Ru(bpz)_3]^{2+}$ in aqueous solution. Dotted lines indicate the laser energies used in this study.

Both the electronic and resonance Raman spectra of $[Ru(bpm)_3]^{2+}$ and $[Ru(bpz)_3]^{2+}$ have been well enough documented and so shall not be discussed in any great detail here.[40−42] However, given the recently published SQM-NCA extending the treatment of this class of complexes to the whole $[Ru(bpm)_3]^{2+}$ or $[Ru(bpz)_3]^{2+}$ ion rather than just a localized Ru−ligand unit, thus offering valuable symmetry information,[37] it is perhaps useful to review the salient points. The visible region of the electronic absorption spectra of $[Ru(bpm)_3]^{2+}$ and $[Ru(bpz)_3]^{2+}$ is dominated by bands in the 20000−25000-cm^{-1} region, shown in Figure 1, which are attributed to $d_\pi \rightarrow \pi^*$ metal−ligand charge-transfer (MLCT) transitions of the type $^1E \leftarrow {}^1A_1$ and are absent in the spectra of the free ligands. As can be seen from Figure 1, excitation at 457.9 nm is close to resonance with the MLCT band of $[Ru(bpm)_3]^{2+}$ and preresonant with that of $[Ru(bpz)_3]^{2+}$; therefore surface-enhanced spectra of $[Ru(bpm)_3]^{2+}$ recorded at 457.9 nm shall be referred to as SERRS, i.e., surface enhancement operating synergistically with a conventional RR process, whereas all other spectra will be considered to be SERS, i.e., lacking the molecular RR process.

The RR spectra of $[Ru(bpm)_3]^{2+}$ and $[Ru(bpz)_3]^{2+}$ are shown in Figures 2 and 3, respectively, and the band wavenumbers, relative intensities, and assignments are listed in Tables 1 and

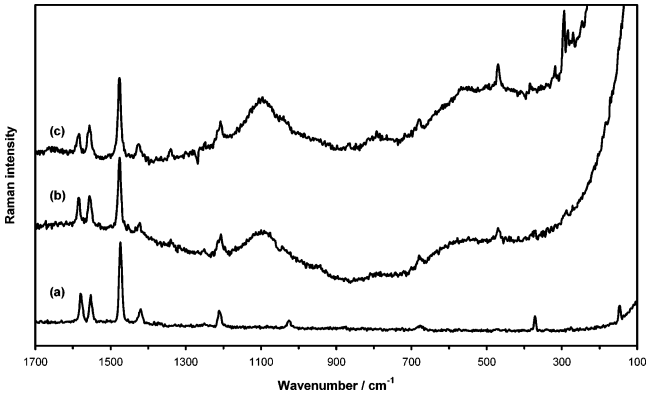

Figure 2. RR spectra of $[Ru(bpm)_3]^{2+}$ excited at (a) 457.9, (b) 488.0, and (c) 514.5 nm.

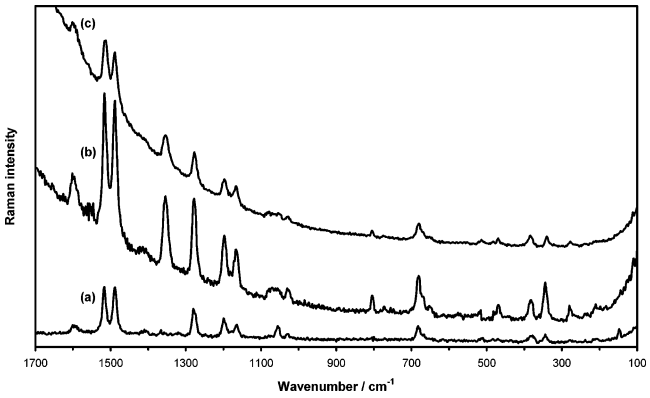

Figure 3. RR spectra of $[Ru(bpz)_3]^{2+}$ excited at (a) 457.9, (b) 476.5, and (c) 488.0 nm.

2, together with the SERS data (vide infra). The strongest bands are attributed to a_1 modes for both species. In the RR spectra of both $[Ru(bpm)_3]^{2+}$ and $[Ru(bpz)_3]^{2+}$ recorded at 457.9 nm, the strongest bands are attributed to the totally symmetric ν(C6C6′) modes followed by S_{8a}, S_{8b}, and δ_{ip}(CH) modes. A number of Raman-allowed modes of e symmetry are also present although are much weaker than the totally symmetric modes in general, with modes involving the S_{19a} symmetry coordinate being strongest. As suggested previously, the dominance of totally symmetric modes accompanied by weak to medium intensity modes indicates that A-term RR scattering governs the relative band intensities within the present excitation range.[43] The lack of a_2 modes in the RR spectra of either species shows that the Herzberg−Teller mechanism is not important in the excitation range employed herein.

Upon alteration of the excitation wavelength, only small changes in the RR spectra of $[Ru(bpm)_3]^{2+}$ are observed. These are most prominent in the 1400−1600-cm^{-1} range. The ν_6 (a_1) ν(C6C6′) mode is strongest under 457.9-nm excitation, when excitation is resonant with the MLCT transition. As the excitation energy is tuned away from resonance, the ν(C6C6′) band decreases in relative intensity with respect to the two strong bands around 1550 cm^{-1}. This is accompanied by a decrease in the intensity of the ν_4 (a_1) S_{8b} mode and an increase in the intensity of the ν_5 (a_1) S_{8a} mode. The resonance enhancement of the ν(C6C6′) mode indicates a strong perturbation of C6C6′ bond in the excited state of $[Ru(bpm)_3]^{2+}$.

The Effect of Adsorption on $[Ru(bpm)_3]^{2+}$ and $[Ru(bpz)_3]^{2+}$. The behavior of the band positions upon adsorption of $[Ru(bpm)_3]^{2+}$ onto the electrode surface is different from that observed previously for $[Ru(bpy)_3]^{2+}$. In most cases in the literature, the bands in the SERS spectrum of $[Ru(bpy)_3]^{2+}$ appear at the same position as those in the RR spectrum, although the relative intensities differ.[43−46] Although many of the vibrational bands of $[Ru(bpm)_3]^{2+}$ lie close to their RR positions in the SERS spectra, a number of bands show important differences. From Figures 2 and 4 and Tables 1 and 3, it can be seen that the S_{8b} band at 1580 cm^{-1}, ν(C6C6′) at

TABLE 1: RR Band Wavenumber Positions (cm^{-1}) and Relative Intensities (Normalized with Respect to the 1472-cm^{-1} Band) for $[Ru(bpm)_3]^{2+}$

	rel intens					
ν	514.5 nm	488.0 nm	457.9 nm	calcd[a]	assignments	
1592			1	1605	ν_{60} (E)	S_{8b}
1580	24	39	36	1604	ν_4 (A_1)	S_{8b}
1558		13		1554	ν_{62} (E)	S_{8a}
1552	42	38	35	1549	ν_5 (A_1)	S_{8a}
1544	9			1547	ν_{63} (E)	S_{8a}
1484	13			1495	ν_{64} (E)	ν(C6C6′)
1472	100	100	100	1496	ν_6 (A_1)	ν(C6C6′)
1421	14	7	22	1428	ν_{65} (E)	S_{19a}, δ_{ip}(C4H)
1336	12	10		1348	ν_8 (A_1)	δ_{ip}(C4H)
1245	4	8	4	1250	ν_{71} (E)	S_{14}
1212	17			1221	ν_{72} (E)	δ_{ip}(C2H), δ_{ip}(C4H)
1203	30	36	26	1227	ν_{10} (A_1)	δ_{ip}(C2H), δ_{ip}(C4H)
1023			20	1026	ν_{13} (A_1)	S_{12}, S_1
946		10		949	ν_{82} (E)	δ_{op}(C2H), δ_{op}(C4H)
862	7			874	ν_{16} (A_1)	S_4, δ_{op}(C6C6′)
802		4		813	ν_{86} (E)	δ_{op}(C3H)
788	9	4		796	ν_{18} (A_1)	S_{6b}
677	12	17	12	674	ν_{19} (A_1)	S_{6a}
475	18	2	4	486	ν_{21} (A_1)	S_{16b}, S_{16a}
466	5	28		465	ν_{95} (E)	S_{16b}
379			1	378	ν_{22} (A_1)	ν(C6C6′)
369			11	372	ν_{97} (E)	ν(C6C6′)
339			2	339	ν_{98} (E)	Chel.def-1, ν(RuN)
315	10			295	ν_{23} (A_1)	S_{16b}
281	11	10	2	283	ν_{99} (E)	S_{16b}
267	5	3	2	249	ν_{24} (A_1)	Chel.def-1
120	62	6		121	ν_{26} (A_1)	S_{16a}, Chel.tor-1

[a] Scaled calculated values from ref 37.

TABLE 2: Effect of Adsorption on Vibrational Wavenumbers (cm^{-1}) and Relative Intensities $[Ru(bpz)_3]^{2+}$ at 457.9 nm

RR		SER S				
ν	rel intens	ν	rel intens	calcd[a]	assignments[a]	
1598	36	1590	59	1593	ν_4 (A_1)	S_{8b}
1514	96	1502	100	1543	ν_5 (A_1)	S_{8a}
1484	100	1482	81	1490	ν_6 (A_1)	S_{19b}, ν(C6C6′)
1409	15	1403	6	1398	ν_{66} (E)	S_{19a}
1397	1	1385	1	1388	ν_7 (A_1)	δ_{ip}(C3H)
1350	83	1342	28	1329	ν_8 (A_1)	δ_{ip}(C5H)
1275	86	1271	27	1263	ν_{10} (A_1)	S_{14}
1193	41	1195	18	1179	ν_{73} (E)	δ_{ip}(C3H), S_{19a}
1163	29	1161	9	1170	ν_{11} (A_1)	S_{19a}, δ_{ip}(C3H)
1075	2	1073	6	1079	ν_{12} (A_1)	S_1
1051	36	1049	19	1047	ν_{77} (E)	S_1, S_{12}
1029	9	1025	9	1030	ν_{79} (E)	S_1
803	3	803	2	802	ν_{86} (E)	S_4, S_{6a}
779	4			797	ν_{18} (A_1)	S_4
681	44	681	33	672	ν_{19} (A_1)	S_{6a}, S_{6b}
666	7			664	ν_{90} (E)	S_{6a}, S_{6b}
651	3	647	6	644	ν_{91} (E)	S_{6b}
508	11	507	1	488	ν_{21} (A_1)	S_{16b}, S_{16a}, δ_{op}(C6C6′)
480	4	485	2	489	ν_{94} (E)	S_{6a}
463	5	467	2	466	ν_{95} (E)	S_{16b}, S_{16a}
381	37	379	10	378	ν_{22} (A_1)	ν(C6C6′), Chel.def-1
341	25	349	5	340	ν_{98} (E)	Chel.def-1, ν(RuN)
275	10	277	1	271	ν_{23} (A_1)	S_{16b}
234	3			253	ν_{24} (A_1)	Chel.def-1
206	11	199	1	196	ν_{101} (E)	ν(RuN)

[a] Scaled calculated values from ref 37.

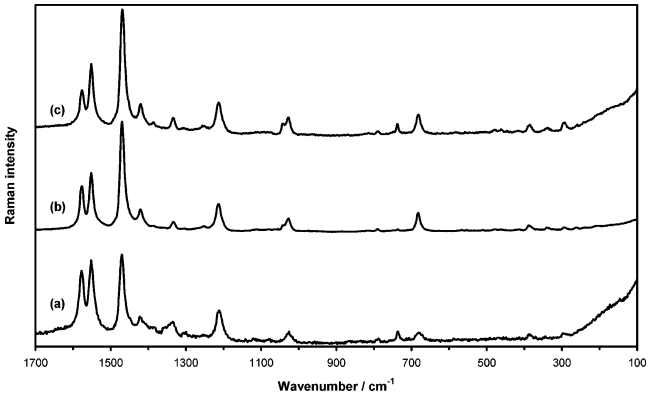

Figure 4. SERS spectra of $[Ru(bpm)_3]^{2+}$ excited at (a) 457.9, (b) 488.0, and (c) 514.5 nm.

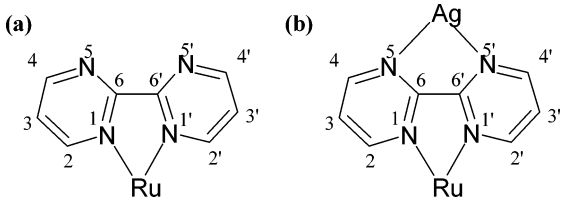

Figure 5. Proposed mode of adsorption for $[Ru(bpm)_3]^{2+}$.

1472 cm^{-1}, δ_{ip}(C4H) at 1336 cm^{-1}, S_{16b} at 467 cm^{-1}, and the Chel.def-1 at 267 cm^{-1} all display large red-shifts, up to 10 cm^{-1}, upon adsorption, whereas the weak S_{19a} band at 1432 cm^{-1}, the S_{14} band at 1242 cm^{-1}, and the δ_{ip}(C2H)/δ_{ip}(C4H) band at 1203 cm^{-1} all move to higher energies by up to 8 cm^{-1}. The 6−7-cm^{-1} red-shift displayed by the ν(C6C6′) mode and the 10-cm^{-1} red-shift of the Chel.def-1 mode are particularly salient. The most likely adsorbate orientation involves one bpm ligand parallel to the surface normal, such that interaction with the electrode surface would occur through the N5 and N5′ atoms. This orientation would effectively lead to the formation of a second chelate ring, shown in Figure 5. Thus, the now bidentate bpm ligand will undergo some structural rearrangement, and it is not unreasonable to suggest that this rearrangement affects mainly the ruthenium−chelate ring and the inter-ring bridging bond. Examples of bpm acting as bidentate or bridging ligand are not uncommon,[47,48] especially with silver atoms.

From Figures 2 and 4, it is evident that adsorption produces only small changes in the relative band intensities for 514.5- and 488.0-nm excitation, and the selective surface enhancement of band intensities is best demonstrated with 457.9-nm excitation. The pair of strong S_{8b} and S_{8a} bands in the 1550−1600-cm^{-1} region are significantly enhanced and are of comparable intensity to the ν(C6C6′) band at 1465 cm^{-1}. The δ_{ip}(C2H)/δ_{ip}(C4H) mode at 1203 cm^{-1} is also enhanced slightly, whereas the heavily mixed ν(C6C6′) mode at 369 cm^{-1} loses intensity upon adsorption. A number of bands not present in the RR spectra are now observed in the SERS spectra. These include the S_{19a}/δ_{ip}(C4H) mixed modes at 1450 and 1416 cm^{-1}. In general, the strongest bands in these spectra are the totally symmetric ones, and in many cases, the bands of e symmetry are reduced in intensity. Furthermore, no a_2 modes are present with appreciable intensity. This is entirely consistent with a dominant EM enhancement mechanism, which would cause totally symmetric modes to be preferentially enhanced over e symmetry modes should the adsorbate be aligned with one of its C_3 or C_2 axes normal to the surface. The exact adsorbate orientation remains somewhat difficult to determine from the enhancement pattern. However, the observed enhancement does not contradict the suggested adsorbate geometry, whereby the $[Ru(bpm)_3]^{2+}$ cation is adsorbed through interaction with the nitrogen atoms on one bpm ligand perpendicular to the surface based on the changes in band positions. However, it should be stressed that this orientation remains only a tentative suggestion. Nevertheless, Sbrana et al.[49] have suggested that the free bpm ligand orientates on silver sols in a similar manner.

The effect of the excitation wavelength on the SERS spectra of $[Ru(bpm)_3]^{2+}$ at −600 mV is shown in Figure 4 and Table 3. Interestingly, the intensity enhancement pattern for 457.9-nm excitation is more pronounced. Here, both the S_{8b} and S_{8a}

TABLE 3: Surface-Enhanced Raman Band Wavenumber Positions (cm^{-1}) and Relative Intensities (Normalized with Respect to the 1465-cm^{-1} Band) for $[Ru(bpm)_3]^{2+}$

	rel intens					
ν	514.5 nm	488.0 nm	457.9 nm	calcd[a]	assignments	
1572	13	21	41	1604	ν_4 (A_1)	S_{8b}
1548	33	33	52	1549	ν_5 (A_1)	S_{8a}
1465	100	100	100	1496	ν_6 (A_1)	ν(C6C6′)
1450	8			1428	ν_{33} (A_2)	S_{19a}, δ_{ip}(C4H)
1416	11	9	11	1428	ν_{65} (E)	S_{19a}, δ_{ip}(C4H)
1406		1		1399	ν_{76} (A_1)	δ_{ip}(C2H)
1382	1		1	1386	ν_{81} (A_1)	δ_{ip}(C2H), δ_{ip}(C3H)
1330	6	5	1	1348	ν_8 (A_1)	δ_{ip}(C4H)
1300			1	1279	ν_{69} (E)	S_{14}
1250	1	1	1	1250	ν_{71} (E)	S_{14}
1209	29	28	49	1227	ν_{10} (A_1)	δ_{ip}(C2H), δ_{ip}(C4H)
1074			3	1082	ν_{76} (E)	S_{19b}
1024	12	12	15	1026	ν_{13} (A_1)	S_{12}, S_1
962	1			974	ν_{81} (E)	δ_{op}(C3H), δ_{op}(C4H)
868	1			874	ν_{16} (A_1)	S_4, δ_{op}(C6C6′)
812		1		813	ν_{86} (E)	δ_{op}(C3H)
785	2	1	2	796	ν_{18} (A_1)	S_{6b}
679	17	17	12	674	ν_{19} (A_1)	S_{6a}
506		1		512	ν_{93} (E)	Chel.def-2
477	1	1		486	ν_{21} (A_1)	S_{16b}, S_{16a}
459	1			465	ν_{95} (E)	S_{16b}
383	6	4	4	372	ν_{22} (A_1)	ν(C6C6′)
337	4		2	339	ν_{23} (A_1)	S_{16b}
287	5	2	1	283	ν_{99} (E)	S_{16b}
257	1	1	2	249	ν_{24} (A_1)	Chel.def-1

[a] Scaled calculated values from ref 37.

modes are clearly enhanced with respect to the ν(C6C6′) mode. Indeed, the intensities of the S_{8b} and S_{8a} bands are found to be the most dependent upon excitation wavelength, and compared with the ν(C6C6′) mode at 1465 cm^{-1}, these modes are strongest in the 457.9-nm spectrum. The S_{8a} mode at 1548 cm^{-1} is weakest in the 488.0-nm spectrum, whereas the S_{8b} mode at 1572 cm^{-1} is weakest in the 514.5-nm spectrum. The δ_{ip}(C2H)/δ_{ip}(C4H) mode at 1212 cm^{-1} is also enhanced, while the ν_{64} (e) ν(C6C6′) mode loses intensity at 457.9 nm. The excitation-dependent enhancement of these modes indicates that, at 457.9-nm excitation, an additional mechanism for enhancement is operational. The intensity ratio of these two bands also changes with excitation wavelength. Should the EM mechanism be solely responsible for the surface enhancement, then the enhancement patterns would not be expected to be excitation wavelength dependent. Thus the presence of CT enhancement at 457.9 nm is proposed. Without an internal standard it is difficult to say whether the CT mechanism is operational for the bands listed above or for the ν(C6C6′) band, which has been used as a reference in Tables 1 and 3. SERS measurements on $[Ru(bpy)_3]^{2+}$ adsorbed on silver surfaces have not displayed vast evidence for an active CT mechanism.[43−46] However, the CT mechanism has been reported for bpm adsorbed on silver sols,[49] $[Re(CO)_3Br(bpm)]$ adsorbed on silver sols via the free nitrogen atoms of the bpm ligand,[50] and $[Co(bpy)_3]^{2+}$ and $[Ni(bpy)_3]^{2+}$ on silver electrodes.[51] Srnova-Sloufova et al. have also reported evidence of the CT mechanism in the SERS of $[Ru(bpy)_3]^{2+}$ on silver colloids.[52]

The effect of adsorption on the Raman spectrum of $[Ru(bpz)_3]^{2+}$ at 457.9 nm is shown in Figure 6 and Table 2. In comparison with $[Ru(bpm)_3]^{2+}$, band shifts upon adsorption are larger for $[Ru(bpz)_3]^{2+}$. However, many of the bands move to a lower wavenumber upon adsorption. The S_{8b} band at 1598 cm^{-1}, the S_{8a} band at 1514 cm^{-1}, the S_{19a} band at 1409 cm^{-1}, and the δ_{ip}(C5H) band at 1350 cm^{-1} are all shifted downward by ca. 12 cm^{-1}. Only the S_{16b}/S_{16a} band at 463 cm^{-1} and the Chel.def-1/ν(RuN) band at 341 cm^{-1} are moved to appreciably

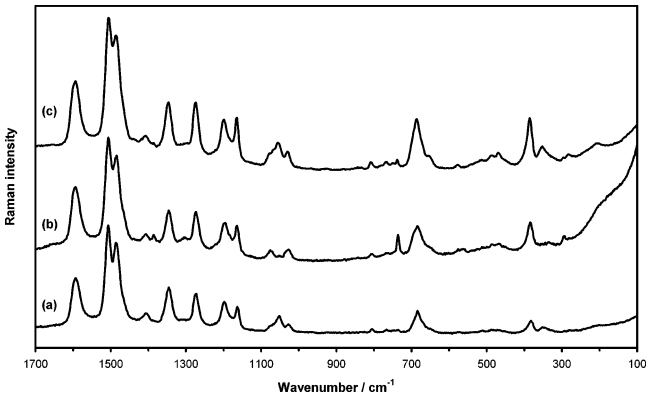

Figure 6. SERS spectra of $[Ru(bpz)_3]^{2+}$ excited at (a) 457.9, (b) 488.0, and (c) 514.5 nm.

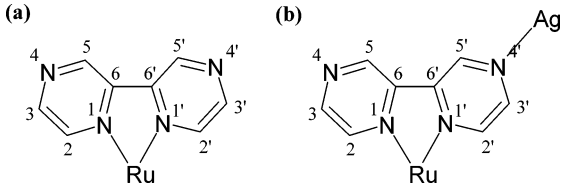

Figure 7. Proposed mode of adsorption for $[Ru(bpz)_3]^{2+}$.

higher wavenumbers upon adsorption. The larger shifts indicate a larger degree of interaction between the $[Ru(bpz)_3]^{2+}$ and the silver surface than that observed for $[Ru(bpm)_3]^{2+}$. This would reflect the different adsorption processes of both cations. The most likely adsorption mechanism for $[Ru(bpz)_3]^{2+}$ is also through the exterior nitrogen atoms, shown in Figure 7. Such an orientation would involve the NNRu axis lying along the surface normal and would result in little steric interaction between the electrode surface and the ligand, contrasting with the case for $[Ru(bpm)_3]^{2+}$. Such an orientation as that shown in Figure 7 would be expected to primarily affect the bonds of the pyrazine moieties, the inter-ring bonds and chelate rings

would not be expected to be significantly perturbed. Therefore, it is especially noteworthy that the S_{19b}/ν(C6C6′) and ν(C6C6′)/Chel.def-1 modes are relatively unperturbed and that the band shifts observed upon adsorption tend to support the proposed model. Lever et al. have observed exciplex formation between silver ions and the peripheral nitrogen atoms of $[Ru(bpz)_3]^{2+}$,[53] while Toma et al. have reported bpz ligands coordinated to three ruthenium ions.[54] Neto et al. have proposed a similar adsorption geometry for the free bpz ligand.[55]

Only small changes in the relative intensities are observed (Figure 6). Similar to the case of $[Ru(bpm)_3]^{2+}$, the most noticeable enhancements are found in the 457.9 nm SERS spectrum. The S_{8b} mode at 1598 cm^{-1} now appears in the SERS spectrum with over half the intensity of the pair of bands between 1470 and 1520 cm^{-1}. The S_{8a} band at 1502 cm^{-1} is also enhanced slightly compared to its counterpart at 1482 cm^{-1}. Elsewhere there appear only small enhancements: the ν(C6C6′)/Chel.def-1 band at 381 cm^{-1} is enhanced compared to the Chel.def-1/ν(RuN) band at 349 cm^{-1}; a distinct shoulder appears on the blue edge of the S_1/S_{12} band at 1051 cm^{-1} in the SERS spectrum, possibly attributable to the S_1 mode. Again, it can be seen from Table 2 that it is the totally symmetric modes of $[Ru(bpz)_3]^{2+}$ that experience the greatest enhancement upon adsorption. Modes of e symmetry that appeared with medium intensity in the RR spectrum, have substantially less intensity in the SERS spectrum. No a_2 modes are present, suggesting that the EM mechanism is dominant, as is the case for $[Ru(bpm)_3]^{2+}$ and $[Ru(bpy)_3]^{2+}$. It is interesting to note the apparent lack of enhancement of the S_{19b}/ν(C6C6′) mode compared to other a_1 modes, especially the S_{8a} and S_{8b} modes. The adsorption geometry proposed in Figure 7 from the band shifts suggests that the C6C6′ bonds contain a larger component parallel to the surface than normal to it. Thus, from the EM surface selection rules modes involving ν(C6C6′) would not be expected to display large enhancements.

Figure 6 shows the effect of excitation wavelength on the SERS spectra of $[Ru(bpz)_3]^{2+}$ at −600 mV. The excitation wavelength exerts very little effect on the SERS spectra of $[Ru(bpz)_3]^{2+}$. The intensity of the S_{8b} band at 1590 cm^{-1} maximizes at 488.0 nm, while the intensity of the S_{19b}/ν(C6C6′) band maximizes at 514.5 nm when compared to the band at 1502 cm^{-1}. The most dramatic resonance effects are observed in the S_{6a}/S_{6b}, S_{6b}, and ν(C6C6′)/Chel.def-1 bands at 683, 653, and 383 cm^{-1} respectively. It would be difficult to argue for the presence of an active CT mechanism based on the wavelength dependence shown in Figure 6 as little wavelength dependence is observed although the S_{19b}/ν(C6C6′) mode is apparently affected by the excitation energy slightly more than other bands.

Effect of Potential on SERS Spectra. SERRS spectra of $[Ru(bpm)_3]^{2+}$ recorded at different potentials are shown in Figure 8 for 457.9-nm excitation. The absolute intensities of all bands attain their maximum values between −500 and −600 mV. Indeed, this is also the case for the absolute intensities in the 488.0- and 514.5-nm excited spectra. Such behavior reflects the increase of surface coverage close to the point of zero charge of polycrystalline silver. The relative intensity of the ν(C6C6′) band at 1465 cm^{-1} in the 457.9-mV spectra, defined with respect to the δ_{ip}(C2H)/δ_{ip}(C4H) band at 1209 cm^{-1}, maximizes around −500 mV. The δ_{ip}(C2H)/δ_{ip}(C4H) band was chosen as it was consistently strong enough to limit errors and was due predominantly to motions involving hydrogen atoms. Should a CT mechanism be present, as indicated by the behavior of the relative intensities upon changing excitation wavelength, it would be expected that a band involving predominantly ν(CH) or δ_{ip}(CH) would be comparatively uninfluenced by the chemical mechanism.[22−24] The relative intensity of the S_{8b} band at 1575 cm^{-1} is also found to be potential dependent, maximizing at −500 mV. The S_{8a} band at 1550 cm^{-1} displays a slight dependence upon applied potential, maximizing between −100 mV and −200 mV. The potential-dependent behavior of the ν(C6C6′) and S_{8b} bands with respect to the δ_{ip}(C2H)/δ_{ip}(C4H) band at 1209 cm^{-1} is shown in Figure 9. At 488.0 nm, the relative band intensity of the ν(C6C6′) band clearly reaches a maximum at −600 mV, whereas the relative intensity of the S_{8b} band is less obviously dependent on potential. The behavior of the ν(C6C6′) and S_{8b} bands at 514.5 nm is similar to that of the 488.0-nm spectra: the relative intensities of the ν(C6C6′) band at 1465 cm^{-1} and the S_{8b} band at 1572 cm^{-1} maximize at potentials slightly more cathodic than −600 and −400 mV, respectively.

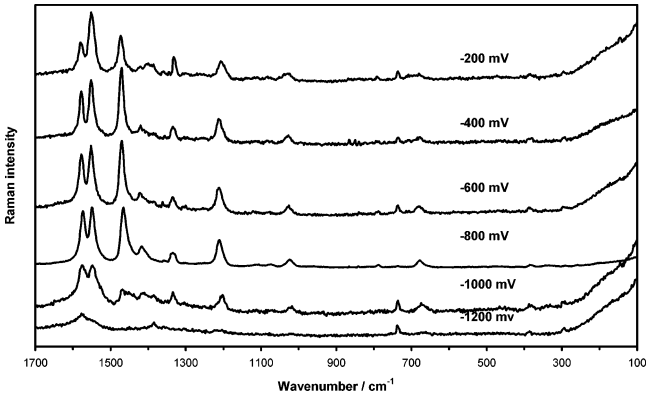

Figure 8. SERRS spectra of $[Ru(bpm)_3]^{2+}$ excited at 457.9 nm as a function of applied potential.

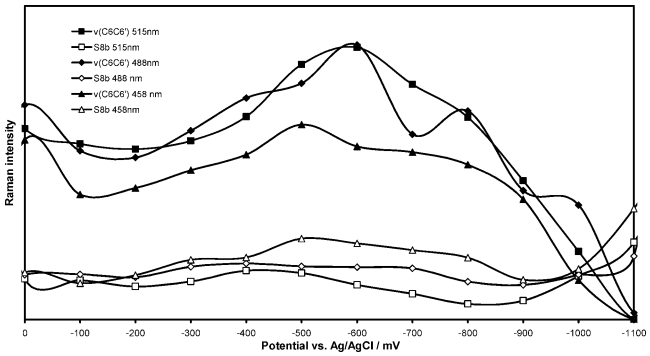

Figure 9. Dependence of relative intensities of SERS bands of $[Ru(bpm)_3]^{2+}$ with applied potential.

The relative intensity-potential profiles (Figure 9) show the potential dependence of the ν(C6C6′) band and, to a lesser extent, the S_{8b} band. It is clear from the raw spectra that the intensity of the ν(C6C6′) band is more potential dependent than the other bands. This potential dependence, accompanied by the wavelength dependent behavior of the SERS spectra, shown in Figure 3, indicate that the ν(C6C6′) mode has the greatest CT activity. From the changes in the potential of maximum intensity, V_{max}, with changes in excitation energy, it has been proposed that the direction of CT involved in the CT mechanism can be determined.[20,21] From Figure 10, it can be seen that the slopes of the excitation energy vs V_{max} plots are different for the ν(C6C6′) and S_{8b} bands, 2.83 eV/V for the ν(C6C6′) band and −2.39 eV/V for the S_{8b} band. Such behavior does not necessarily indicate a breakdown in the CT model of Rubim and co-workers. Different directions of CT have been observed before.[56,57] From Figure 10, it is possible to say that for the

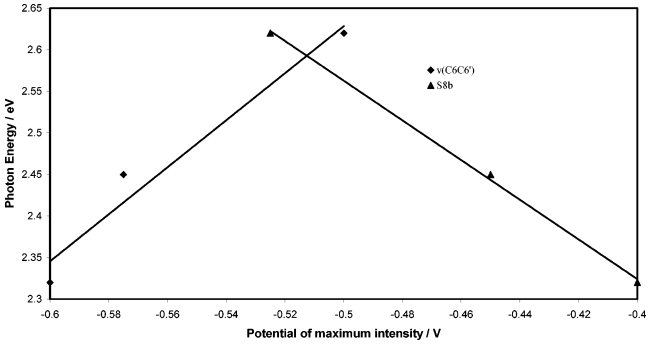

Figure 10. Potential of maximum intensity vs excitation energy plots for $[Ru(bpm)_3]^{2+}$.

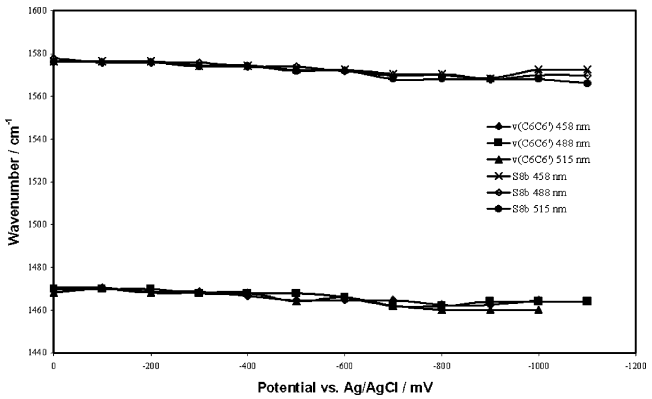

Figure 11. Variation of band energies with applied potential for $[Ru(bpm)_3]^{2+}$.

ν(C6C6′) mode the direction of charge is from the electrode to the adsorbate. This is in good agreement with that observed by Corio and Rubim in $[Co(bpy)_3]^{2+}$ and $[Ni(bpy)_3]^{2+}$.[51] According to Corio and Rubim for MLCT, the dependence on V_{max} with excitation energy can be modeled by the equation

$$E_{excite} = a(V_{red} - V_{max}) \quad (1)$$

where E_{excite} is the excitation energy, V_{red} is the reduction potential of the acceptor orbital involved in the CT process, and a is an electric field shielding coefficient. From the slope and intercept of the plot in Figure 10, a V_{red} value of −1.42 V is obtained. This is in qualitative agreement with the value of −1.24 V for the third reduction of $[Ru(bpm)_3]^{2+}$.[58] It is not just the band intensities that are perturbed by a change in applied potential. Figure 11 shows the potential dependence of the position of the 1465- and 1572-cm^{-1} bands. Slopes are typically of the order of ca. 8 cm^{-1}/V. The energy of the 1548-cm^{-1} band remains relatively constant over the applied potential range. A sharp increase in the plot of the 1572-cm^{-1} band can be seen between applied potentials of −900 and −1000 mV.

The reduction potentials of $[Ru(bpm)_3]^{2+}$ in acetonitrile have been given as −0.87, −1.04, and −1.24 V vs Ag/AgCl.[58] Thus in the −0.9 to −1.2 V potential region changes may be expected in the position of the bands. It can be seen from Figure 8 that no such dramatic changes occur. Nevertheless, from Figure 11, it can be seen that, upon application of more cathodic potentials, the S_{8b} and ν(C6C6′) bands gradually decrease in wavenumber and generally reach a minimum around −0.9 V before stabilizing. The gradual red-shift in band energy can be attributed to either Stark shifts or to a change in the strength of interaction with the silver surface. The apparent stabilization may be evidence of the formation of the first reduction product, $[Ru(bpm)_3]^{+}$. Corio and Rubim noted that for the first reduction of

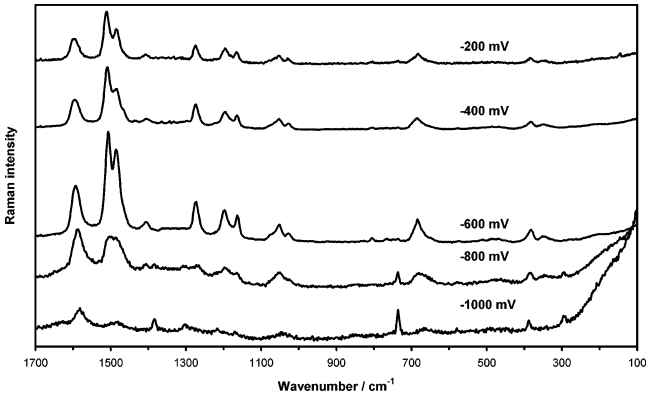

Figure 12. SERS spectra of $[Ru(bpz)_3]^{2+}$ excited at 457.9 nm as a function of applied potential.

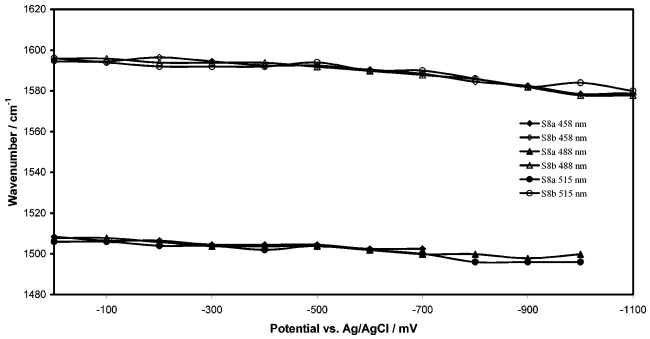

Figure 13. Variation of band energies with applied potential for $[Ru(bpz)_3]^{2+}$.

$[Co(bpy)_3]^{2+}$, the transferred electron may be localized on the central metal ion.[51] However, they concluded this possibility unlikely due to large changes in band positions in their SERS spectra at different potentials. Changes of 10 cm^{-1} upon the first reduction of $[Ru(bpy)_3]^{2+}$ in acetonitrile have also been observed by Virdee and Hester.[46] It can be seen from Figure 8 that, despite the lack of large changes in the positions of the most intense bands, the spectra do show a change on going from −0.8 to −1.0 V. An attenuation of the intensities of many bands, most dramatically and most notably that of the ν(C6C6′) band, can be seen as more negative potentials than −900 mV are applied. The peaks around 1550 cm^{-1} show a considerable degree of broadening and a small feature around 1440 cm^{-1} appears. As is suggested for the case of a transferred electron localized on one ligand, the SERS spectrum of $[Ru(bpm)_3]^{+}$ may contain bands due to bpm and bpm$\bullet^{-}$ moieties. This may be the reason for the observed broadening although the large reduction in signal-to-noise ratio, partially due to the onset of degradation of the electrode surface upon the application of highly cathodic potentials, precludes any definitive analysis.

The SERS spectra of $[Ru(bpz)_3]^{2+}$ recorded at 457.9 nm over a wide potential range are shown in Figure 12. The absolute intensities show similar behavior with a change in potential to those of $[Ru(bpm)_3]^{2+}$, maximizing around −600 mV. This was found to also be the case at other excitation wavelengths, similar to the case of $[Ru(bpm)_3]^{2+}$. In general, the positions of the bands show only small variations with applied potential. Band positions are generally found to occur at lower energies at more cathodic-applied voltages. The largest potential dependence is displayed by the S_{8a} mode, at 1502 cm^{-1}, and the S_{8b} mode at 1590 cm^{-1}. These bands are shown in Figure 13. The slopes of these plots are ca. 10 cm^{-1}/V for the S_{8a} mode and 17 cm^{-1}/V for the S_{8b} mode and are of similar order to those observed for $[Ru(bpm)_3]^{2+}$.

The reduction potentials of $[Ru(bpz)_3]^{2+}$ have been reported to occur at −0.83, −0.98, and −1.22 V vs Ag/AgCl.[59] Similar to $[Ru(bpm)_3]^{2+}$, no significant changes in the positions of the bands are observed in the potential region of the first two reduction processes. However, in the case of $[Ru(bpz)_3]^{2+}$, broadening of the intense bands between 1400 and 1500 cm^{-1} occurs at −0.8 V as opposed to −0.9 V, observed for $[Ru(bpm)_3]^{2+}$. Although this cannot be taken as direct evidence of the first reduction product, the onset of spectral degradation occurs at more anodic potentials for $[Ru(bpz)_3]^{2+}$, possibly due to the easier reduction of $[Ru(bpz)_3]^{2+}$ compared to $[Ru(bpm)_3]^{2+}$.

The behavior of the relative band intensities with applied potential is difficult to ascertain. Between 0 and −700 mV, little potential dependence is observed. At 457.9 nm, the S_{19b}/ν(C6C6′) and S_{8a} bands, at 1482 and 1502 cm^{-1} respectively, exhibit a slight potential dependence. From Figure 12, it can be seen that the relative intensity of the former band maximizes around −800 mV, whereas the latter is strongest around −400 mV. The potential of maximum intensity of the S_{8a} band shifts anodically to −500 mV at 488.0 nm and ca. −600 mV at 514.5 nm, whereas the S_{19b}/ν(C6C6′) band maximizes around −700 mV at 488.0 nm and −600 mV at 514.5 nm. Excitation energy−V_{max} plots then give slopes of 1.9 eV/V and −3 eV/V for the S_{8a} and S_{19b}/ν(C6C6′) bands, respectively. It could be argued here that the S_{19b}/ν(C6C6′) band is CT active with a direction of CT from adsorbate to metal. However, this is in direct contrast to the directions observed for the ν(C6C6′) mode of $[Ru(bpm)_3]^{2+}$ and for $[Co(bpy)_3]^{2+}$ and $[Ni(bpy)_3]^{2+}$.[51] Furthermore, the positions of V_{max} are somewhat ill-defined for $[Ru(bpz)_3]^{2+}$ (e.g., Figure 12) due to the lack of clear potential dependence in the relative intensities. Thus, such an excitation energy−potential plot cannot be relied upon as an indication of the nature of the CT mechanism for $[Ru(bpz)_3]^{2+}$. This observation, along with the fact that the relative intensities of $[Ru(bpz)_3]^{2+}$ are inherently less potential dependent, makes it clear that $[Ru(bpz)_3]^{2+}$ is substantially less CT active than $[Ru(bpm)_3]^{2+}$. Therefore, it is concluded that the CT mechanism is not important for $[Ru(bpz)_3]^{2+}$.

The reasons for the different CT activity of $[Ru(bpm)_3]^{2+}$ and $[Ru(bpz)_3]^{2+}$ are not initially clear, and it is suggested that this difference may lie in the adsorption orientations. The bidentate nature of the $[Ru(bpm)_3]^{2+}$ adsorption to the silver surface may lead to a more effective overlap of the adsorbate and silver orbitals. $[Ru(bpz)_3]^{2+}$ is suggested to adsorb through only one nitrogen atom, and so the interaction between surface and $[Ru(bpz)_3]^{2+}$ would be weaker. It is especially pertinent that it is the ν(C6C6′) mode of $[Ru(bpm)_3]^{2+}$ that displays the greatest CT activity. The inter-ring bond would presumably be more susceptible to charge transfer with the proposed adsorption of $[Ru(bpm)_3]^{2+}$ rather than that of $[Ru(bpz)_3]^{2+}$.

The differences in adsorption modes would be particularly relevant if the CT activity arose from "SERS-active sites" such as surface defects or Ag_4^+-type clusters rather than from a band structure description invoking the Fermi level of the electrode. Surface defects, adatoms, or Ag_4^+ clusters would lend themselves to binding to $[Ru(bpm)_3]^{2+}$ better than 10−100-nm scale surface roughness features, although this remains speculative.

Conclusions

The SERS of $[Ru(bpm)_3]^{2+}$ and $[Ru(bpz)_3]^{2+}$ are reported for the first time at a roughened silver electrode. It was found in both cases that totally symmetric modes were preferentially enhanced, indicating a dominant EM enhancement mechanism. Large changes in band positions attendant upon adsorption indicate a strong degree of complexation of both $[Ru(bpm)_3]^{2+}$ and $[Ru(bpz)_3]^{2+}$ to the electrode surface. This is to be contrasted with the behavior of $[Ru(bpy)_3]^{2+}$, which gives bands that are unperturbed by adsorption.[43] From changes in band positions upon adsorption and, to a lesser extent, enhancement patterns, it was possible to infer a likely adsorption orientation, especially for $[Ru(bpm)_3]^{2+}$. Modes associated with the inter-ring bond and five-membered ruthenium chelate ring show the greatest change upon adsorption indicating the formation of a new, five-membered chelate ring involving the silver surface and the free nitrogen atoms of one bipyrimidine ligand upon adsorption of $[Ru(bpm)_3]^{2+}$. Bands involving the inter-ring stretch of $[Ru(bpz)_3]^{2+}$ were not found to be as sensitive to adsorption, and an adsorption through the nitrogenous lone pair electrons to the silver surface was suggested.

There were no large changes in the appearance of the SERS spectra of $[Ru(bpm)_3]^{2+}$ and $[Ru(bpz)_3]^{2+}$ in the 0.0 to −0.9 V potential range, indicating a lack of detectable electrochemical processes. In both cases, the overall intensity of the SERS spectra were found to maximize around −600 mV, corresponding to the point of zero charge and thus a maximum in complex surface concentration. A sharp deterioration in the quality of the SERS spectra could be observed at potentials where the first reduction products of $[Ru(bpm)_3]^{2+}$ and $[Ru(bpz)_3]^{2+}$ are expected to be formed. Not only did the signal-to-noise ratio decrease but also certain bands were shown to broaden significantly. Unfortunately, the reduction products could not be identified, partially due to the broadening of spectral features and partially due to the onset of degradation on the silver surface due to the application of an increasingly cathodic potential.

Despite the lack of major changes in the SERS spectra of $[Ru(bpm)_3]^{2+}$, the relative intensity of the ν(C6C6′) band was found to be dependent on both the excitation wavelength and the applied potential. The fact that it was possible to find a potential of maximum intensity for the relative intensity of this band and that this potential changed with excitation wavelength was ascribed to an active CT mechanism for this band operating synergistically with the EM mechanism. From plots of potentials of maximum intensity against excitation energy it was possible to determine the direction of CT as electrode to adsorbate, in good agreement with previously reported behavior of $[Co(bpy)_3]^{2+}$ and $[Ni(bpy)_3]^{2+}$.[51] No such CT activity was observed in $[Ru(bpz)_3]^{2+}$, and this behavior is suggested to arise from the different modes of adsorption of the two complexes, which is reflected in the different changes in band positions upon adsorption. Bpm has been previously observed to adsorb more strongly on silver than bpz.[55]

Acknowledgment. One of us (B.D.A.) would like to thank the University of Dundee for a University Scholarship.

References and Notes

(1) Haque, S. A.; Tachibana, Y.; Willis, R. L.; Moser, J.-E.; Grätzel, M.; Klug, D. R.; Durrant, J. R. *J. Phys. Chem. B* **2000**, *104*, 538.

(2) Kalyanasundaram, K.; Gratzel, M. *Coord. Chem. Rev.* **1998**, *77*, 347.

(3) Lee, K. W.; Slinker, J. D.; Gorodetsky, A. A.; Flores-Torres, S.; Abruna, H. D.; Houston, P. L.; Malliaras, G. G. *Phys. Chem. Chem. Phys.* **2003**, *5*, 2706.

(4) Miao, W. J.; Bard, A. J. *Anal. Chem.* **2003**, *75*, 5825.

(5) Weatherly, S. C.; Yang, I. V.; Armistead, P. A.; Thorp, H. H. *J. Phys. Chem. B* **2003**, *107*, 372.

(6) Leone, A. M.; Brennaman, M. K.; Tibodeau, J. D.; Papanikolas, J. M.; Murray, R. W.; Thorp, H. H. *J. Phys. Chem. B* **2003**, *107*, 6469.

(7) Albrecht, M. G.; Creighton, J. A. *J. Am. Chem. Soc.* **1977**, *99*, 5215.

(8) Jeanmaire, D. L.; Vanduyne, R. P. *J. Electroanal. Chem.* **1977**, *84*, 1.
(9) Graham, D.; Mallinder, B. J.; Whitcombe, D.; Watson, N. D.; Smith, W. E. *Anal. Chem.* **2002**, *74*, 1069.
(10) Graham, D.; Fruk, L.; Smith, W. E. *Analyst* **2003**, *128*, 692.
(11) Cao, Y. W. C.; Jin, R. C.; Mirkin, C. A. *Science* **2002**, *297*, 1536.
(12) Sulk, R. A.; Corcoran, R. C.; Carron, K. T. *Appl. Spectrosc.* **1999**, *53*, 954.
(13) McHugh, C. J.; Smith, W. E.; Lacey, R.; Graham, D. *Chem. Commun.* **2002**, 2514.
(14) McHugh, C. J.; Keir, R.; Graham, D.; Smith, W. E. *Chem. Commun.* **2002**, 580.
(15) Rodger, C.; Rutherford, V.; Broughton, D.; White, P. C.; Smith, W. E. *Analyst* **1998**, *123*, 1823.
(16) White, P. C. *Sci. Justice* **2000**, *40*, 113.
(17) Creighton, J. A. *Advances in Spectroscopy*; Clark, R. J. H., Hester, R. E., Eds.; J. Wiley & Sons: Chichester, 1988; Vol. 16.
(18) Otto, A.; Mrozek, I.; Grabhorn, H.; Akemann, W. *J. Phys.: Condens. Matter* **1992**, *4*, 1143.
(19) Campion, A.; Kambhampati, P. *Chem. Soc. Rev.* **1998**, *27*, 241.
(20) Lombardi, J. R.; Birke, R. L.; Sanchez, L. A.; Bernard, I.; Sun, S. C. *Chem. Phys. Lett.* **1984**, *104*, 240.
(21) Rubim, J. C.; Corio, P.; Ribeiro, M. C. C.; Matz, M. *J. Phys. Chem.* **1995**, *99*, 15765.
(22) Arenas, J. F.; Fernandez, D. J.; Soto, J.; Lopez-Tocon, I.; Otero, J. C. *J. Phys. Chem. B* **2003**, *107*, 13143.
(23) Arenas, J. F.; Tocon, I. L.; Otero, J. C.; Marcos, J. I. *J. Phys. Chem.* **1996**, *100*, 9254.
(24) Arenas, J. F.; Woolley, M. S.; Otero, J. C.; Marcos, J. I. *J. Phys. Chem.* **1996**, *100*, 3199.
(25) Kambhampati, P.; Foster, M. C.; Campion, A. *J. Chem. Phys.* **1999**, *110*, 551.
(26) Kambhampati, P.; Campion, A. *Surf. Sci.* **1999**, *428*, 115.
(27) Kambhampati, P.; Child, C. M.; Foster, M. C.; Campion, A. *J. Chem. Phys.* **1998**, *108*, 5013.
(28) Kambhampati, P.; Child, C. M.; Campion, A. *J. Chem. Soc., Faraday Trans.* **1996**, *92*, 4775.
(29) Zylka, G.; Otto, A. *Surf. Sci.* **2001**, *475*, 118.
(30) Bjerneld, E. J.; Foldes-Papp, Z.; Kall, M.; Rigler, R. *J. Phys. Chem. B* **2002**, *106*, 1213.
(31) Kneipp, K.; Kneipp, H.; Itzkan, I.; Dasari, R. R.; Feld, M. S. *J. Phys.: Condens. Matter* **2002**, *14*, R597.
(32) Kneipp, K.; Kneipp, H.; Itzkan, I.; Dasari, R. R.; Feld, M. S. *Chem. Rev.* **1999**, *99*, 2957.
(33) Habuchi, S.; Cotlet, M.; Gronheid, R.; Dirix, G.; Michiels, J.; Vanderleyden, J.; De Schryver, F. C.; Hofkens, J. *J. Am. Chem. Soc.* **2003**, *125*, 8446.
(34) Hunziker, M.; Ludi, A. *J. Am. Chem. Soc.* **1977**, *99*, 7370.
(35) Crutchley, R. J.; Lever, A. B. P. *Inorg. Chem.* **1982**, *21*, 2276.
(36) Evans, I. P.; Spencer, A.; Wilkinson. G. *J. Chem. Soc., Dalton Trans.* **1973**, 204.
(37) Alexander, B. D.; Dines, T. J. *Inorg. Chem.* **2004**, *43*, 342.
(38) Frisch, M. J.; Trucks, G. W.; Schlegel, H. B.; Scuseria, G. E.; Robb, M. A.; Cheeseman, J. R.; Zakrzewski, V. G.; Montgomery, J. A., Jr.; Stratmann, R. E.; Burant, J. C.; Dapprich, S.; Millam, J. M.; Daniels, A. D.; Kudin, K. N.; Strain, M. C.; Farkas, O.; Tomasi, J.; Barone, V.; Cossi, M.; Cammi, R.; Mennucci, B.; Pomelli, C.; Adamo, C.; Clifford, S.; Ochterski, J.; Petersson, G. A.; Ayala, P. Y.; Cui, Q.; Morokuma, K.; Malick, D. K.; Rabuck, A. D.; Raghavachari, K.; Foresman, J. B.; Cioslowski, J.; Ortiz, J. V.; Stefanov, B. B.; Liu, G.; Liashenko, A.; Piskorz, P.; Komaromi, I.; Gomperts, R.; Martin, R. L.; Fox, D. J.; Keith, T.; Al-Laham, M. A.; Peng, C. Y.; Nanayakkara, A.; Gonzalez, C.; Challacombe, M.; Gill, P. M. W.; Johnson, B. G.; Chen, W.; Wong, M. W.; Andres, J. L.; Head-Gordon, M.; Replogle, E. S.; Pople, J. A. *Gaussian 98*, revision A.5; Gaussian, Inc.: Pittsburgh, PA, 1998.
(39) Pulay, P.; Fogarasi, G.; Pongor, G.; Boggs, J. E.; Vargha, A. *J. Am. Chem. Soc.* **1983**, *105*, 7037.
(40) Danzer, G. D.; Kincaid, J. R. *J. Phys. Chem.* **1990**, *94*, 3976.
(41) Balk, R. W.; Stufkens, D. J.; Crutchley, R. J.; Lever, A. B. P. *Inorg. Chim. Acta* **1982**, *64*, L49.
(42) Tait, C. D.; Donohoe, R. J.; DeArmond, M. K.; Wertz, D. W. *Inorg. Chem.* **1987**, *26*, 2754.
(43) Dines, T. J.; Peacock, R. D. *J. Chem. Soc., Faraday Trans. 1* **1988**, *84*, 3445.
(44) Edmiston, M. J.; Peacock, R. D. *Spectrochim. Acta, Part A* **1996**, *52*, 191.
(45) Stacy, A. M.; Van Duyne, R. P. *Chem. Phys. Lett.* **1983**, *102*, 365.
(46) Virdee, H. R.; Hester, R. E. *J. Phys. Chem.* **1984**, *88*, 451.
(47) Krejcik, M.; Vlcek, A. A. *Inorg. Chem.* **1992**, *31*, 2390.
(48) Nallas, G. N. A.; Jones, S. W.; Brewer, K. J. *Inorg. Chem.* **1996**, *35*, 6974.
(49) Sbrana, G.; Neto, N.; Munizmiranda, M.; Nocentini, M. *J. Phys. Chem.* **1990**, *94*, 3706.
(50) Vlckova, B.; Matejka, P.; Vanoutersterp, J. W. M.; Snoeck, T. L.; Stufkens, D. J. *Inorg. Chem.* **1994**, *33*, 2132.
(51) Corio, P.; Rubim, J. C. *J. Phys. Chem.* **1995**, *99*, 13217.
(52) Srnova-Sloufova, I.; Vlckova, B.; Snoeck, T. L.; Stufkens, D. J.; Matejka, P. *Inorg. Chem.* **2000**, *39*, 3551.
(53) Lever, A. B. P.; Seymour, P.; Auburn, P. R. *Inorg. Chim. Acta* **1988**, *145*, 43.
(54) Toma, H. E.; Santos, P. S.; Lever, A. B. P. *Inorg. Chem.* **1988**, *27*, 3850.
(55) Neto, N.; MunizMiranda, M.; Sbrana, G. *J. Phys. Chem.* **1996**, *100*, 9911.
(56) Corio, P.; Rubim, J. C. *J. Raman Spectrosc.* **1997**, *28*, 235.
(57) Corio, P.; Temperini, M. L. A.; Santos, P. S.; Rubim, J. C. *Langmuir* **1999**, *15*, 2500.
(58) Rillema, D. P.; Allen, G.; Meyer, T. J.; Conrad, D. *Inorg. Chem.* **1983**, *22*, 1617.
(59) Crutchley, R. J.; Lever, A. B. P. *J. Am. Chem. Soc.* **1980**, *102*, 7128.